Inorganic Chemistry
Article
Cite This: Inorg. Chem. XXXX, XXX, XXX–XXX
pubs.acs.org/IC

Stabilizing Copper for CO_2 Reduction in Low-Grade Electrolyte

Jingfu He,[†] Aoxue Huang,[†] Noah J. J. Johnson,[†] Kevan E. Dettelbach,[†] David M. Weekes,[†] Yang Cao,[†] and Curtis P. Berlinguette*[,†,‡,§]

[†]Department of Chemistry, The University of British Columbia, 2036 Main Mall, Vancouver, British Columbia V6T 1Z1, Canada
[‡]Department of Chemical & Biological Engineering, The University of British Columbia, 2360 East Mall, Vancouver, British Columbia V6T 1Z3, Canada
[§]Stewart Blusson Quantum Matter Institute, The University of British Columbia, 2355 East Mall, Vancouver, British Columbia V6T 1Z4, Canada

Supporting Information

ABSTRACT: We demonstrate herein a CO_2 reduction electrocatalyst regeneration strategy based on the manipulation of the $Cu(0)/Cu^{2+}$ equilibrium with high concentrations of ethylenediaminetetraacetic acid (EDTA). This strategy enables the sustained performance of copper catalysts in distilled and tap water electrolytes for over 12 h. The deposition of common electrolyte impurities such as iron, nickel, and zinc is blocked because EDTA can effectively bind the metal ions and negatively shift the electrode potential of M/M^{n+}. The Cu/Cu^{2+} redox couple is >600 mV more positive than the other metal ions and therefore participates in an equilibrium of dissolution and redeposition from and to the electrode in high concentrations of EDTA. These dynamic equilibria serve to further regenerate the surface copper catalyst to prevent the deactivation of catalytic sites. On the basis of this strategy, we show that >95% of initial hydrocarbon production activity can be maintained for 12 h in $KHCO_3$ (99% purity) enriched distilled water and 6 h in $KHCO_3$ (99% purity) enriched tap water.

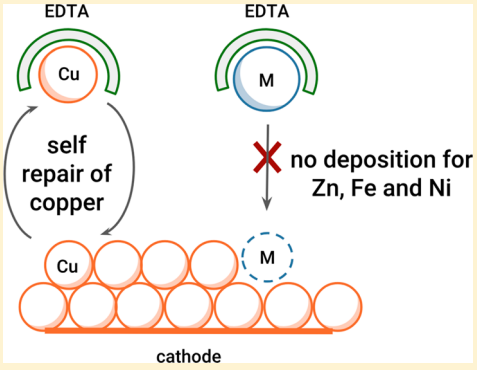

INTRODUCTION

Electrochemical CO_2 reduction technologies require electrocatalysts that can operate continuously for extended time periods.[1−4] CO_2 reduction reaction (CO_2RR) electrocatalysts are therefore typically tested in ultrapure electrolytes in an effort to avoid catalyst poisoning from metal impurities.[5−11] Copper catalysts are an appealing class of CO_2RR electrocatalysts owing to their ability to produce hydrocarbons, but they are particularly susceptible to poisoning. Indeed, copper systems significantly lose catalytic activity in <1 h when electrolysis is performed in an untreated electrolyte constituting Milli-Q water and ACS standard >99% purity $KHCO_3$.[3,12] Trace amounts of impurities in the electrolyte and buildup of carbonaceous byproducts on the catalyst surface are purported to be responsible for catalyst deactivation.[12−14] This situation presents a conflict for achieving long-term stability while using an inexpensive electrolyte for practical electrolysis.

There are many ways to address catalyst deactivation for electrolytic and photolytic processes beyond CO_2RR (e.g., oxygen evolution,[15−17] oxygen reduction,[18] hydrogen evolution[19]). The strategy of electrolyte tuning/modification to recover and maintain sustained electrolysis has resulted in manganese-, cobalt-, and nickel-oxide-based water oxidation catalysts that corrode and redeposit under catalytic conditions.[16,17,20−26] This reactivity has proven effective for providing prolonged activity for oxygen evolution catalysis, but this strategy has yet to be applied to electrochemical CO_2 reduction systems.

Efforts to maintain sustained CO_2RR activity by copper catalysts typically focus on preventing electrodes from impurity poisoning from electrolyte. For example, pretreatment of an electrolyte consisting of Milli-Q water and ACS standard >99% purity $KHCO_3$ by predeposition of electrolyte impurities onto a sacrificial electrode or by Chelex ion exchange can enhance the effective lifetime of a catalyst several-fold; however, the reagent and time costs are high.[3,12,27−29] Oxide-derived copper and gold electrocatalysts reported by Kanan and co-workers in 2012 were demonstrated to be less susceptible to poisoning from electrolyte impurities compared with copper and gold planar electrodes due to their large surface area and can stably produce CO and HCOOH for extended periods (~7 h).[7,30] A self-cleaning strategy that blocks the deposition of impurities and carbon byproducts was proposed by Wang and co-workers in order to maintain the stability of a copper catalyst.[4] Therein, palladium atoms predeposited on a copper surface appeared to induce a morphological and compositional restructuring of the copper surface, serving to continually refresh the catalyst and maintain electrochemical selectivity. The faradaic efficiency (FE) for hydrocarbon products in that case was stable over 5 h in pre-electrolyzed $KHCO_3$ electrolyte (Milli-Q water and

Received: August 15, 2018

DOI: 10.1021/acs.inorgchem.8b02311
Inorg. Chem. XXXX, XXX, XXX–XXX

99.7% $KHCO_3$). Despite these collective advances, there remains no reported case of a copper catalyst that can mediate hydrocarbon evolution in low- or medium-grade electrolytes (e.g., distilled water or tap water containing up to 99% purity electrolyte salt).

We show herein a catalyst regeneration strategy that blocks the deposition of certain metallic impurities (e.g., Ni, Fe, Zn) and prevents byproduct accumulation which inhibits electrocatalytic performance by simultaneously re-forming the copper catalyst surface layer during CO_2 electrolysis conditions (Scheme 1). This result is achieved by the addition of a high concentration (>1000 mg/L) of the common metal chelator ethylenediaminetetraacetic acid (EDTA)[31] in the electrolyte solution. Lower concentrations of EDTA (~1 mg/L) in the electrolyte have been reported to extend the lifetime of gold catalysts in ultrapure electrolyte, but this strategy was reported not to improve the lifetime of copper catalysts.[27] EDTA has a strong binding affinity (log $\beta_{M\text{-}EDTA}$ ~ 16−18) for four metal ions Cu^{2+}, Fe^{3+}, Ni^{2+}, and Zn^{2+} present in our local water supply and readily forms the metal complexes in solution.[27] The standard electrode potential of M^{2+}/M^0 for Cu is at least 600 mV positive compared to the relevant Fe, Ni, and Zn redox couples, so it will be less likely to totally dissolve in the EDTA-containing electrolyte during CO_2RR but rather will form a dynamic equilibrium of Cu/Cu^{2+}/EDTA-Cu. The leaching and redeposition of copper can be encouraged by a high concentration of EDTA in the electrolyte, so that the active surface of the electrocatalyst is constantly refreshed. Using this strategy, we are able to maintain >95% of the activity of a copper catalyst toward CO_2-to-hydrocarbon reduction for 12 h in distilled water with ACS grade $KHCO_3$ (99% purity), and up to 6 h stability in untreated tap water. This discovery showcases the possibility of manipulating the equilibria of metals and metal−organic complexes to regenerate CO_2 reduction catalysts.

Scheme 1. Proposed Mechanism for the Prolonged Stability of Copper Electrocatalysts towards CO_2-to-Hydrocarbon Reduction as a Result of the Addition of Ethylenediaminetetraacetic Acid (EDTA) in the Electrolyte Solution[a]

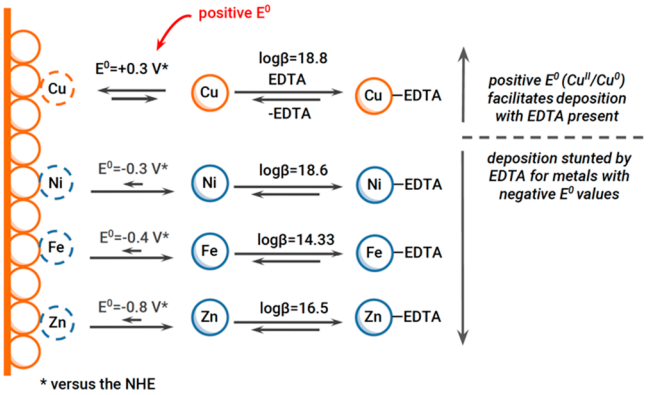

[a]EDTA binds all four metal ions (Cu^{2+}, Ni^{2+}, $Fe^{2+/3+}$, Zn^{2+}) with high binding affinity (log $\beta_{M\text{-}EDTA}$ ~ 16−18) and negatively shifts the deposition potential; thus, only copper has a sufficiently positive reduction potential to enable redeposition of the metal on the electrode surface under an applied voltage and continuously regenerate the surface catalytic sites. The deposition of impurity metals (Fe, Ni, Zn) is blocked by the presence of EDTA, thereby preventing catalyst poisoning. Reduction potentials are vs NHE.

EXPERIMENTAL SECTION

CO_2 reduction experiments were performed in a gastight two-compartment glass H-cell with a proton exchange membrane (Nafion 117; Fuel Cell Store) as a separator. Each compartment contained 50 mL of 0.5 M $KHCO_3$ electrolyte with various concentrations of EDTA. The quality of the electrolyte is denoted by the type of water used in each experiment, which is either Milli-Q (MQ) water, distilled (DI) water, or tap (TAP) water. The H-cell was rinsed before each series of experiments with a 1:1 mixture of concentrated HNO_3/H_2SO_4 in order to regulate the impurity levels of the experiments. Prior to starting the experiment, the H-cell was rinsed with MQ water three times and with electrolyte once. Long-term stability testing was performed at −1.3 V vs RHE without *iR* compensation, as are all voltages reported in this research. The resistance is 8 ± 0.5 Ω for all systems. This potential was chosen as the optimal CO_2-to-hydrocarbon potential region.[32,33] The copper catalyst was prepared by electrochemical deposition of copper onto a carbon cloth (see Supporting Information).[34−36] The dendritic morphology of copper prepared by this method was reported by Reller to be an effective hydrocarbon production catalyst.[34] The total loading amount of as-prepared copper on carbon cloth was ~0.003 mmol/cm^2 based on UV−vis absorption titration experiments. The active area of the copper catalyst/carbon samples was 1 cm^2 for all the electrochemical tests in this study. The experiments monitoring copper equilibrium were halted every half hour in the first 2 h and subsequently every 1 h to measure the copper loading on the carbon cloth by X-ray fluorescence (XRF) and copper dissolution in electrolyte by UV−vis spectroscopy.

RESULTS AND DISCUSSION

Electrochemical reduction of CO_2 to CO, CH_4, and C_2H_4 on dendritic copper electrocatalysts was tested in electrolytes with three different impurity levels (MQ, DI or TAP electrolyte) and four different additive choices (without EDTA, 1 mg/L EDTA, 1 g/L EDTA, or 1 g/L EDTA + 0.025 mM $CuCl_2$) (Figure 1). A high-purity electrolyte was prepared from MQ water and (99.997%) K_2CO_3. A medium-purity electrolyte was prepared from DI water and (99%) $KHCO_3$, and a low-purity electrolyte was prepared from untreated TAP and (99%) $KHCO_3$. The electrolytes all contained K^+ concentrations of 0.5 M and were all presaturated with gaseous CO_2 to reach a pH of 6.9 prior to electrolysis. The metal-ion concentrations for each of the three electrolytes were quantified by inductively coupled plasma optical emission spectroscopy (ICP-OES and ICP-MS; see Supporting Information).

The electrocatalytic performance in MQ electrolyte was in accordance with previous literature reports (~20−30% FE for each of methane and ethylene; ~10% FE for CO).[32] The overall current density (j) was stable at 38 mA cm^{-2} during 6 h of operation; however, the total FE for CO_2 reduction products gradually decreased by about one-third during this time (Figure 1a). Electrochemical CO_2 reduction in DI electrolyte displayed an initial performance similar to that of the MQ electrolyte, but the performance rapidly declined over the course of the experiment (FE = <10% for CH_4 and <3% for C_2H_4 and CO after 6 h of continuous operation; Figure 1b). In the TAP electrolyte, the electrocatalyst was immediately deactivated and no CO_2 reduction products were detected after merely 1 h of electrolysis (Figure 1c). These experiments demonstrate the widely documented vulnerability of copper toward electrocatalyst poisoning and deactivation while operating in non-ultrapure electrolytes. Adding low concen-

DOI: 10.1021/acs.inorgchem.8b02311
Inorg. Chem. XXXX, XXX, XXX−XXX

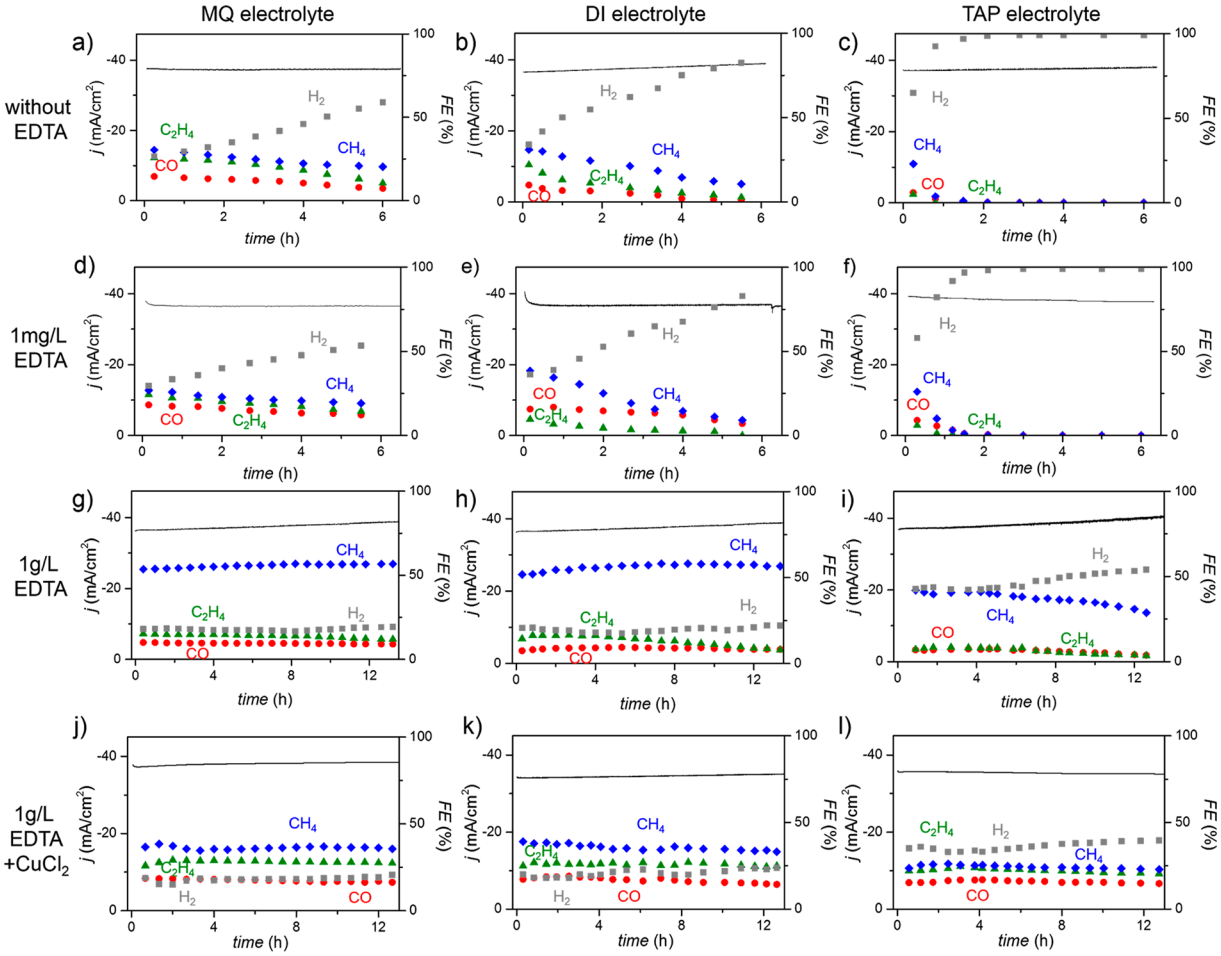

Figure 1. Time-resolved current densities (j, black line) and faradaic efficiencies (FEs, dots) for CO_2 reduction products CO, CH_4, and C_2H_4 on dendritic copper catalysts supported on carbon cloth in a CO_2-saturated 0.5 M $KHCO_3$ electrolyte either (a–c) without EDTA, (d–f) with 1 mg/L EDTA, (g–i) with 1000 mg/L EDTA in solution, or (j–l) with 1000 mg/L EDTA and 0.025 mM $CuCl_2$ in solution and composed of (a, d, g, and j) Milli-Q (MQ) water and 99.997% K_2CO_3, (b, e, h, and k) distilled (DI) water and 99% $KHCO_3$, and (c, f, i, and l) tap (TAP) water and 99% $KHCO_3$. Electrolytes with 1000 mg/L EDTA are labeled as X_{EDTA} electrolyte (X = MQ, DI, or TAP) throughout this paper. The liquid products of formic acid, methanol, and ethanol were quantified by ^1H NMR, but the amounts produced were <3%; we discontinued monitoring for liquid products as shown in Figure S4. The resistances are 8 ± 0.5 Ω for all systems and not compensated for in our system.

trations of EDTA (1 mg/L) did not influence the lifetime of copper catalyst in the three types of electrolyte (Figures 1d–f), and the decline in electrocatalytic stability is consistent with those samples in which EDTA was not present. Considering that the highest impurity concentration detected in MQ electrolyte is 3.7 nM for Zn, 3 orders of magnitude lower than the EDTA concentration, these data indicate that impurity poisoning is not the only reason for the observed deactivation process.

Electrocatalytic CO_2 reduction stability was enhanced in all three electrolyte compositions by the addition of 1000 mg/L EDTA to the electrolyte solution while holding all other parameters at parity (Figure 1g–i; see Figures S1, S2, and S3 for performance and stability data). The initial FEs for CH_4, C_2H_4, and CO production were ∼50%, ∼15%, and ∼10%, respectively, for both the MQ_{EDTA} and DI_{EDTA} electrolytes. These values remained virtually constant throughout 12 h of electrolysis at $j \sim 40$ mA cm^{-2} (Figure 1g,h). The current densities for all the different electrolytes and EDTA concentrations were approximately the same, and the changes in current densities over 12 h electrolysis were less than 10%, thereby providing a useful platform for understanding catalyst stability and the competitive reactions between HER and CO_2RR. Stable FEs of 40% and 10% were also recorded for CH_4 and C_2H_4, respectively, over 6 h in TAP_{EDTA} and declined only slightly after this time (Figure 1i). This result is in stark contrast to the almost immediate decline in electrocatalytic performance witnessed in the TAP electrolyte (Figure 1c,f). The observations in TAP_{EDTA} are the first demonstration of copper-catalyzed CO_2 reduction with sustained electrocatalytic performance in a low-grade electrolyte (TAP).

The X-ray diffraction (XRD) pattern and X-ray photoelectron spectroscopy (XPS) for the copper electrocatalyst did not reveal apparent changes in peak intensities and positions after 12 h of continuous operation (Figures S4a and S5). The electrolytes were assessed postelectrolysis by ^1H NMR spectroscopy (Figure S4b) to reveal an intensity change of <1% and no chemical shift of the EDTA hydrogen peaks (at 3.2 and 3.6 ppm) after 12 h of continuous operation. In a separate control experiment, copper electrolysis in 0.5 M KCl electrolyte containing 1000 mg/L EDTA was tested at the same voltage under N_2 flow (Figures S6 and S7). H_2 was the only product detected by GC and NMR analysis. The negligible change in the EDTA concentration of the catholyte

DOI: 10.1021/acs.inorgchem.8b02311
Inorg. Chem. XXXX, XXX, XXX–XXX

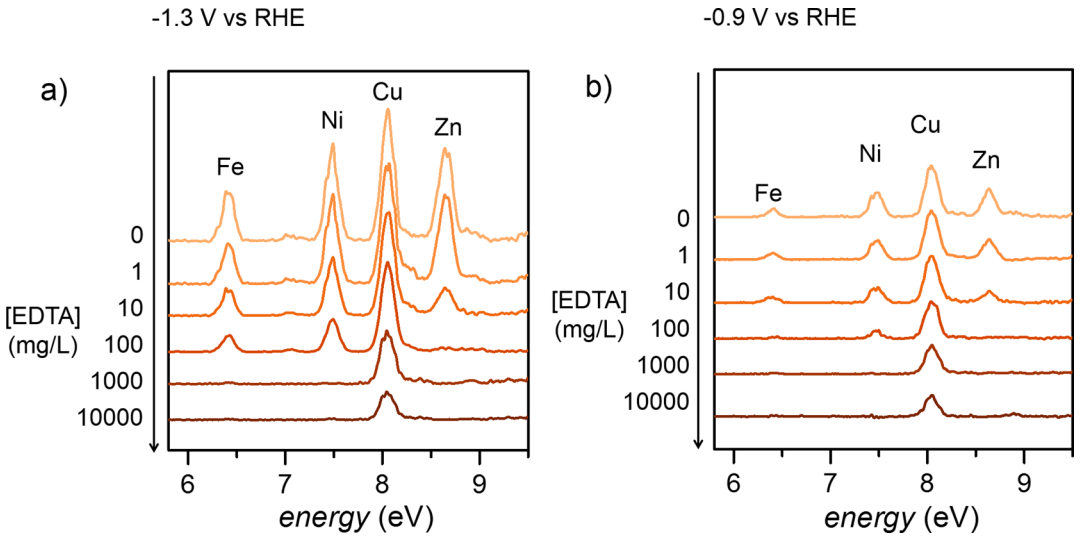

Figure 2. (a) XRF spectra of a carbon cloth electrode after 4 h of electrodeposition at −1.3 V vs RHE in DI_{EDTA} electrolyte containing 0.1 mM $Fe(NO_3)_3$, $Ni(NO_3)_2$, $Cu(NO_3)_2$, and $Zn(NO_3)_2$ with EDTA at various concentrations (from top to bottom: 0, 1, 10, 100, 1000, 10000 mg/L). (b) XRF spectra of a carbon cloth electrode after 4 h of electrodeposition at −0.9 V vs RHE in DI_{EDTA} electrolyte containing 0.1 mM $Fe(NO_3)_3$, $Ni(NO_3)_2$, $Cu(NO_3)_2$, and $Zn(NO_3)_2$ with EDTA at various concentrations (from top to bottom: 0, 1, 10, 100, 1000, and 10 000 mg/L).

(<2%) and the lack of any EDTA on the anolyte side rule out the possibility of EDTA acting as a sacrificial agent during electrocatalysis.

One significant effect of adding >1000 mg/L EDTA to the electrolyte is a change in selectivity of the copper catalyst. The copper catalyst operating in ultrapure electrolyte produces similar amounts of C_2H_4 and CH_4, while the CH_4/C_2H_4 product ratio obtained in MQ_{EDTA}, DI_{EDTA}, and TAP_{EDTA} electrolyte containing 1000 mg/L EDTA was increased to 5. We rationalize that this change in selectivity was due to the dissolution of copper atoms from the electrode to the electrolyte (vide infra). It was found that the addition of 0.025 mM $CuCl_2$ to the electrolyte solution containing EDTA was sufficient to prevent the selectivity change of copper electrolysis. The product selectivity for electrochemical CO_2 reduction under these conditions (MQ_{EDTA} + Cu^{2+}, DI_{EDTA} + Cu^{2+} and TAP_{EDTA} + Cu^{2+}) is similar to reports of catalysts working in ultrapure electrolytes and is consistent over 12 h (Figure 1j–l).

As listed in Table S2, the concentrations of Fe, Ni, and Zn impurities are 40−800 nM in TAP water and 0.05−3.7 nM in MQ water. The EDTA concentration of 1000 mg/L (3.4 mM) is 3 magnitudes higher than impurities in TAP water, while 1 mg/L (3.4 μM) EDTA is 3 magnitudes higher than impurities in MQ water. The stability of copper is nonetheless dramatically different in the two environments. It is notable that, in Surendanth's report, 1 mg/L of EDTA in the electrolyte sufficiently binds metal-ion impurities in the electrolyte but does not improve the lifetime of copper catalysts for CO_2 reduction.[27] We have determined that preventing metal ions from depositing onto the catalysts does not account for the increased catalyst stability in our EDTA electrolytes. Electrodeposition at −1.3 V was performed on a copper foil (99.99%) electrode for 12 h in untreated TAP and TAP_{EDTA} electrolytes. The electrode was tested postelectrolysis for surface contamination by X-ray photoelectron spectroscopy (XPS; Figure S8). The resulting spectrum for the TAP experiment showed clear peaks corresponding to Ni and Zn on the electrode surface. These peaks are absent from the copper sample, even in 1 mg/L EDTA. Although metal-ion impurities cannot be deposited on the copper catalyst regardless of the low concentration of EDTA, the FTIR spectrum of copper foil after 12 h of operation with 1 mg/L EDTA shows new peaks at 1400 and 1700 cm^{-1} (Figure S9), which are not observed for copper operating in 1000 mg/L EDTA. The peak at ∼1400 cm^{-1} likely corresponds to CO_3 and HCO_3; however, this peak remains when the foil is rinsed with water. This indicates that there might be some chemical bond between copper and carbonate. The peak at around ∼1700 cm^{-1} is probably similar to some intermediate products of CO_2 reduction, such as CHO*.[37] As mentioned in previous research studies, carbon-based compounds can block the surface and deactivate the catalyst, indicating that an important contribution of the large concentration of EDTA is to prevent surface blocking.

Metal deposition experiments were performed with different concentrations of EDTA to quantitatively determine the influence of EDTA in the dynamics of metal-ion leaching/deposition. The metal impurity concentration in our electrolytes is below our limits of detection (0.2 μmol/cm^2 for XRF). Therefore, 0.1 mM $Fe(NO_3)_3$, $Ni(NO_3)_2$, $Cu(NO_3)_2$, and $Zn(NO_3)_2$ were purposely added to a DI electrolyte to artificially induce much greater levels of inhibitive impurities compared with the electrolytes used thus far. These impurities are known to immediately deactivate electrocatalytic copper surfaces under applied bias (Figure S10).[12,27] The deposition of impurity metals (e.g., Fe, Ni, Zn) on an electrode surface is blocked in electrolyte containing different concentrations of EDTA (0, 1, 10, 100, 1000, or 10 000 mg/L) as shown in Figure 2. An electrodeposition potential of −1.3 V vs RHE was applied, and XRF was used to monitor the quantity of metal deposited onto the electrode surface (Figure 2a).[38,39] All four metals were readily deposited on the electrode when EDTA was absent from the electrolyte. The deposition of Zn is hindered when the EDTA concentration is increased to 10 mg/L. No Zn is deposited, and the deposition of Fe and Ni is significantly reduced with an EDTA concentration of 100 mg/L. Only copper is deposited when the EDTA concentration is 1000 mg/L or greater. This is reasonable, because in EDTA-

DOI: 10.1021/acs.inorgchem.8b02311
Inorg. Chem. XXXX, XXX, XXX−XXX

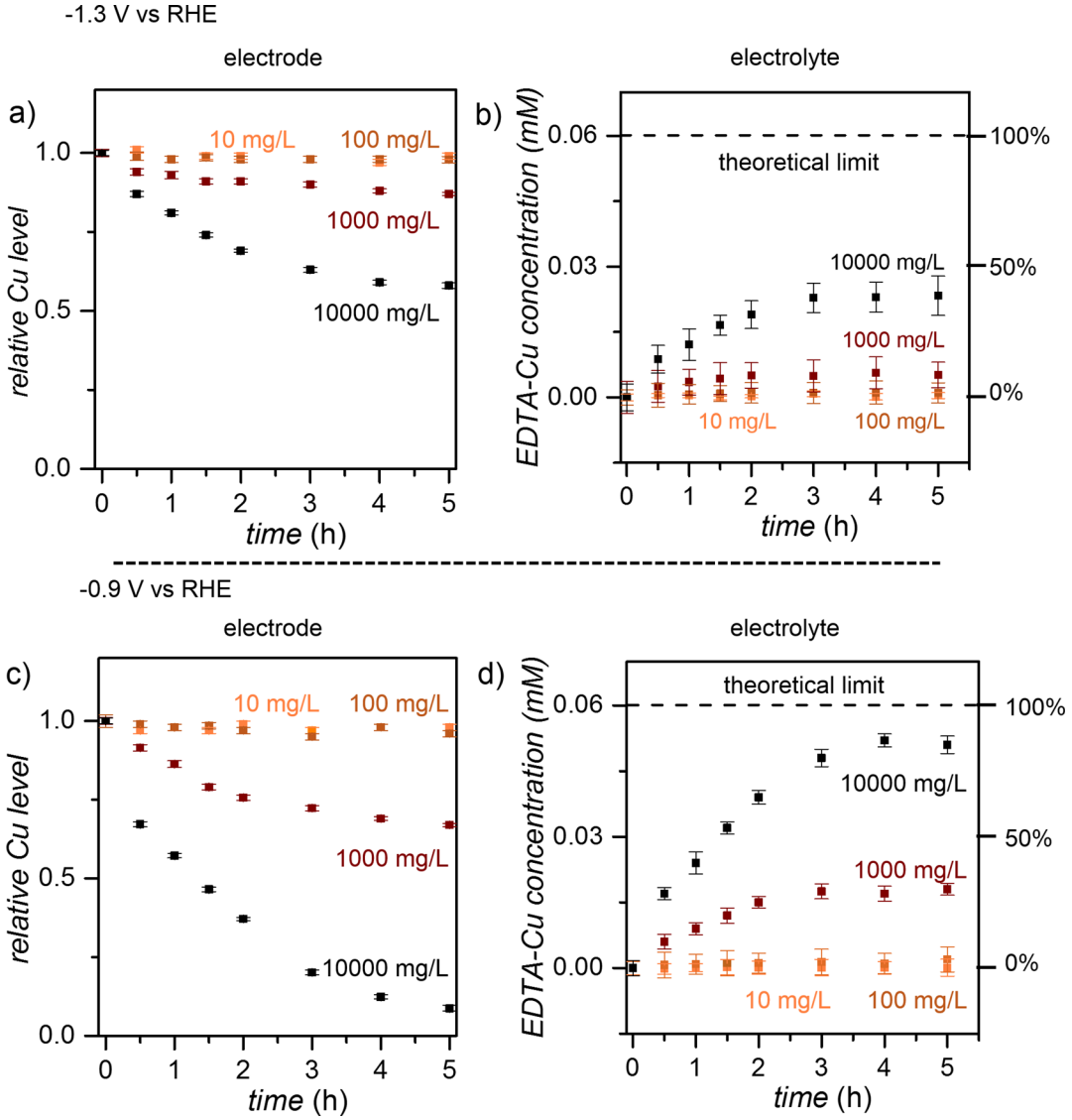

Figure 3. (a) Relative concentration of Cu at the electrode surface (determined by normalized XRF) and (b) the concentration of Cu^{2+}-EDTA complex in the solution (determined by UV−vis spectroscopy) as measured over time during CO_2 reduction electrocatalysis at −1.3 V vs RHE in DI_{EDTA} electrolyte with different concentrations of EDTA. (c) The relative concentration of Cu at the electrode surface and (d) the concentration of Cu^{2+}-EDTA complex in the solution as measured over time during CO_2 reduction electrocatalysis at −0.9 V vs RHE in DI_{EDTA} electrolyte with different concentrations of EDTA.

containing electrolyte, the electrodeposition potentials of all metal ions are negatively shifted with lower free metal-ion concentrations. These experiments were repeated at an electrodeposition potential of −0.9 V (the lower voltage limit at which hydrocarbon production from CO_2RR is observed),[40] with similar deposition blocking order of Zn > Fe > Ni > Cu with increasing EDTA concentration. It is worth noting that the deposition of transition metal ions still occurs with a low concentration of EDTA (100 mg/L) at more positive operating voltage.

The leaching and redeposition equilibrium of metal ions can be understood with the two equations listed below:

$$E = E^\circ + \frac{RT}{ZF}\log(C_{M^{n+}}) \quad (1)$$

$$\beta = \frac{[\mathrm{EDTA} - \mathrm{M}]}{[\mathrm{EDTA}^{n-}][M^{n+}]} \quad (2)$$

where E° is the standard electrode potential of M^{n+}/M, R is the universal gas constant, T is the temperature, F is the Faraday constant, Z is the number of electrons transferred in the half-reaction, and β is the formation constant. The electrodeposition potential of metal ions is related to the free metal-ion concentration and the standard electrode potential. In a standard CO_2RR experiment without EDTA, all metal ions have more positive electrode potentials than CO_2RR, thereby resulting in deposition of all metal impurities on the surface of the electrode. The EDTA binding ratio with the transition metal ions studied in our research is almost 100%; thus, the concentration of free metal ions falls as EDTA is added to negatively shift the M/M^{n+} electrode potential. This effect is not apparent when the EDTA concentration is lower than the total concentration of metal ions in the electrolyte. Indeed, Figure 2a,b shows that electrodeposition occurs in electrolytes containing 0−10 mg/L EDTA. When the EDTA concentration surpasses the initial concentration of metal ions,

DOI: 10.1021/acs.inorgchem.8b02311
Inorg. Chem. XXXX, XXX, XXX−XXX

the concentration of free metal ions would be decreased by magnitudes. On the basis of the rough calculation of a 1:1 EDTA to metal ions ratio in eqs 1 and 2, the shifted electrode potential would still follow the same order of Zn, Fe, Ni, Cu, from negative to positive, which is consistent with the blocking order observed in Figure 2. When the EDTA concentration is increased to one magnitude higher than the metal ions in electrolyte (in our case 1000 mg/L EDTA vs 0.1 mM Fe^{3+}, Ni^{2+}, Zn^{2+}), the metals are no longer deposited at the surface. This can be rationalized as the electrode potential of M/M^{n+} being negatively shifted by >0.5 V in accordance with eqs 1 and 2. The applied potential will also influence the equilibrium of M/M^{n+}. In the electrodeposition experiment, Fe and Ni deposition at the surface of the electrode is effectively suppressed at −0.9 V with 100 mg/L EDTA, while at −1.3 V the ions can still be quickly deposited on the electrode. The voltage range that can prohibit the deposition of metal is not exactly the same with the prediction from eqs 1 and 2, because CO_2RR and HER act as competing reactions and the resistance is not compensated in our system.

Copper is a unique metal species in this environment in that it cannot be fully leached nor is completely insoluble with high concentrations of EDTA present in the electrolyte. Instead, it forms a Cu/Cu^{2+}/EDTA-Cu equilibrium, which we consider to be crucial for the regeneration of catalyst. The effect of EDTA concentration on this Cu/Cu^{2+}/EDTA-Cu equilibrium was experimentally established in a DI electrolyte to confirm the theoretical prediction by monitoring relative copper levels on the electrode and in the electrolyte by XRF and UV−vis spectroscopy (Figures S11 and S12), respectively, under CO_2RR conditions (applied bias of −1.3 V vs RHE) for 5 h (Figure 3a,b). The XRF signal was stable during electrolysis in electrolytes containing 100 mg/L EDTA or less, indicating that no copper was lost from the electrode surface to the electrolyte. The UV−vis spectra also showed no detectable Cu^{2+}-EDTA in the electrolyte at these concentrations of EDTA. A detectable dissolution of copper occurs when the concentration of EDTA is 1000 mg/L or greater. Increasing EDTA concentrations to 10 000 mg/L results in a ∼40% loss of copper from the electrode surface after 2 h, as indicated by complementary signals in the XRF and the UV−vis spectra. These signals stabilize after 3 h inferring the establishment of an equilibrium between copper on the electrode surface and copper(II) in the electrolyte. To further support this copper dissolution and redeposition process, we performed electrolysis at −1.3 V vs RHE for 6 h at an electrode where a blank carbon cloth electrode (1 cm^2) was placed adjacent to the working copper/carbon cloth electrode (1 cm^2). This experiment led to the dissolution of copper from the working electrode and a subsequent redeposition on the carbon cloth electrode (see SEM images in Figure S13). An equilibrium is also reached within ∼3 h at lower applied potentials (−0.9 V); however, the position of equilibrium is shifted toward the electrolyte at this less negative voltage (Figure 3c,d). This is also consistent with our prediction based on eqs 1 and 2.

The dissolution and redeposition of copper on electrode introduced by EDTA in the electrolyte can also be confirmed by the morphological changes upon the copper catalyst surface in scanning electron microscopy (SEM) images. We sought to qualify any surface changes caused by EDTA by examining a typical copper electrocatalyst by SEM before and after 12 h CO_2 electrolysis in either DI or DI_{EDTA} (Figure 4a−c). The as-prepared copper on carbon cloth sample exhibited large

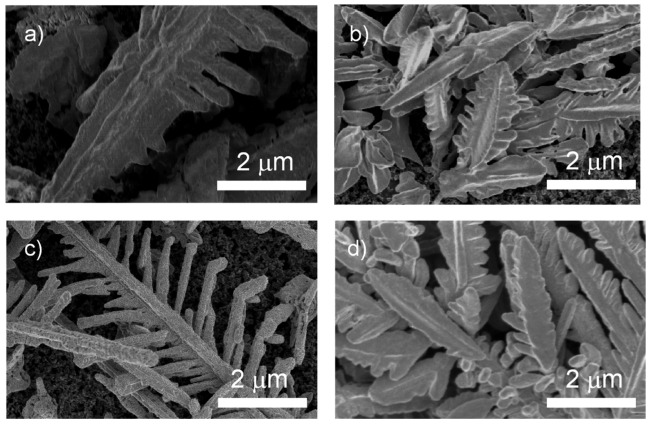

Figure 4. SEM micrographs of Cu electrocatalysts on carbon cloth: (a) as-prepared, (b) after operating in DI electrolyte, (c) after operating in DI_{EDTA} electrolyte, and (d) after operating in DI_{EDTA} with additional 0.025 mM $CuCl_2$. SEM images were collected after 12 h operating at −1.3 V vs RHE.

clusters with branch-like assemblies consistent with dendritic electrodeposited copper (Figure 4a). The smooth surface morphology and thick branches of the catalyst did not change significantly after operating for 12 h in DI electrolyte (Figure 4b). By contrast, electrolysis in DI_{EDTA} electrolyte resulted in noticeable corrosion of both trunk and branches of the dendritic structures (Figure 4c). Also apparent were small additional clusters on the substrate indicating simultaneous copper redeposition and dissolution (Figure S14). This observation is consistent with our XRF data which shows the copper signal decreasing for the first 2 h by 20% and then remaining constant. This change in morphology of the copper catalyst surface also correlates to a difference in CO_2 reduction product selectivity when using either DI or DI_{EDTA} electrolyte (Figure 1b,h). After 12 h of electrolysis, the copper catalyst in DI electrolyte produced CH_4 and C_2H_4 with FEs of 30% and 25%, respectively, whereas the catalyst in DI_{EDTA} electrolyte produced CH_4 and C_2H_4 with FEs of 60% and >10%, respectively. The addition of 0.025 mM $CuCl_2$ to the electrolyte solution containing EDTA was sufficient to shift the equilibrium position toward the electrode surface such that the copper loading on the electrocatalyst surface remained constant from the outset of electrolysis (Figures S15 and S16). Furthermore, the additional copper ions added to the electrolyte prior to electrolysis had the effect of maintaining a more consistent catalyst morphology (Figure 4d). The product selectivity for electrochemical CO_2 reduction under these conditions (DI_{EDTA} + Cu^{2+} and TAP_{EDTA} + Cu^{2+}) is similar to reports of catalysts working in ultrapure electrolytes and is consistent over 12 h (Figure 1k,l).

A threshold EDTA concentration of ∼1000 mg/L is required to achieve long-term stability for Cu catalyst, as indicated by the huge stability difference in low- and high-concentration EDTA electrolytes regardless of the impurity level (Figure 1). A very similar threshold EDTA concentration of 100−1000 mg/L is observed by the introduction of a leaching−redeposition process of copper, as shown in Figures 2−4. These results suggest that this newly established Cu/Cu^{2+} equilibrium created by high concentrations of EDTA is crucial for the long-term stability of the Cu catalyst. For low EDTA concentrations (1 mg/L) that cannot shift the equilibrium, there is little mass exchange between Cu^{2+} in electrolyte and

DOI: 10.1021/acs.inorgchem.8b02311
Inorg. Chem. XXXX, XXX, XXX−XXX

Cu metal on electrode; therefore, no surface structure regeneration occurs. For high EDTA concentrations (1 g/L), a large amount of copper first dissolves into the electrolyte and then forms a dissolution/deposition equilibrium to regenerate the surface active sites. We can estimate from these results that ~0.3% of total copper is leached from the catalyst surface per minute at the onset of electrolysis at −1.3 V with 1000 mg/L EDTA in the electrolyte. Assuming the dissolution kinetics do not change significantly at equilibrium, this estimate suggests that 0.3% of the copper catalyst is refreshed every minute during electrocatalysis. This rapid mass exchange of copper between the electrode and electrolyte allows for the maintenance of a poison-free catalyst surface.

CONCLUSIONS

This study presents an electrocatalyst regeneration strategy that prolongs the lifetime of copper on carbon cloth electrocatalysts toward CO_2 electroreduction to hydrocarbon products while operating in non-ultrapure electrolytes (e.g., distilled or tap water with reagent grade bicarbonate salt). The addition of 1000 mg/L EDTA into the electrolyte solution has the effect of scavenging impurities and inhibiting catalyst blocking from byproducts while constantly regenerating the copper catalyst surface (as demonstrated by XRF and UV−vis data). This effect can primarily be attributed to the differences in reduction potential across a series of transition metal ions (Cu, Ni, Fe, Zn) that are known to bind EDTA. This work demonstrates a tangible strategy to repair electrocatalysts by manipulating the equilibrium of metal/metal ions with a common chelation agent.

ASSOCIATED CONTENT

Supporting Information

The Supporting Information is available free of charge on the ACS Publications website at DOI: 10.1021/acs.inorgchem.8b02311.

XRD patterns, SEM images, NMR spectra, and CO_2 electrochemical reduction performances (PDF)

AUTHOR INFORMATION

Corresponding Author

*E-mail: cberling@chem.ubc.ca.

ORCID

Jingfu He: 0000-0002-7639-0151
Aoxue Huang: 0000-0003-2507-0198
Noah J. J. Johnson: 0000-0002-0721-3186
Kevan E. Dettelbach: 0000-0002-7789-2129
Yang Cao: 0000-0001-8636-7919
Curtis P. Berlinguette: 0000-0001-6875-849X

Notes

The authors declare no competing financial interest.

ACKNOWLEDGMENTS

The authors are grateful to the Canadian Natural Science and Engineering Research Council (RGPIN 337345-13), Canadian Foundation for Innovation (229288), Canadian Institute for Advanced Research (BSE-BERL-162173), and Canada Research Chairs for financial support. K.E.D. was supported by an NSERC PGS-D scholarship. A.H. was supported by the University of British Columbia with a Four Year Doctoral Fellowship (4YF).

REFERENCES

(1) Costentin, C.; Robert, M.; Savéant, J.-M. Catalysis of the electrochemical reduction of carbon dioxide. *Chem. Soc. Rev.* **2013**, *42*, 2423−2436.

(2) Qiao, J.; Liu, Y.; Hong, F.; Zhang, J. A review of catalysts for the electroreduction of carbon dioxide to produce low-carbon fuels. *Chem. Soc. Rev.* **2014**, *43*, 631−675.

(3) Hori, Y. Electrochemical CO_2 reduction on metal electrodes. In *Modern Aspects of Electrochemistry*;Springer: New York, 2008; pp 89−189.

(4) Weng, Z.; Zhang, X.; Wu, Y.; Huo, S.; Jiang, J.; Liu, W.; He, G.; Liang, Y.; Wang, H. Self-cleaning catalyst electrodes for stabilized CO_2 reduction to hydrocarbons. *Angew. Chem., Int. Ed.* **2017**, *56*, 13135−13139.

(5) Asadi, M.; Kim, K.; Liu, C.; Addepalli, A. V.; Abbasi, P.; Yasaei, P.; Phillips, P.; Behranginia, A.; Cerrato, J. M.; Haasch, R.; et al. Nanostructured transition metal dichalcogenide electrocatalysts for CO_2 reduction in ionic liquid. *Science* **2016**, *353*, 467−470.

(6) He, J.; Dettelbach, K. E.; Salvatore, D. A.; Li, T.; Berlinguette, C. P. High-throughput synthesis of mixed-metal electrocatalysts for CO_2 reduction. *Angew. Chem., Int. Ed.* **2017**, *56*, 6068−6072.

(7) Chen, Y.; Li, C. W.; Kanan, M. W. Aqueous CO_2 reduction at very low overpotential on oxide-derived Au nanoparticles. *J. Am. Chem. Soc.* **2012**, *134*, 19969−19972.

(8) Roberts, F. S.; Kuhl, K. P.; Nilsson, A. High selectivity for ethylene from carbon dioxide reduction over copper nanocube electrocatalysts. *Angew. Chem., Int. Ed.* **2015**, *54*, 5179−5182.

(9) Ma, M.; Trześniewski, B. J.; Xie, J.; Smith, W. A. Selective and efficient reduction of carbon dioxide to carbon monoxide on oxide-derived nanostructured silver electrocatalysts. *Angew. Chem., Int. Ed.* **2016**, *55*, 9748−9752.

(10) Clark, E. L.; Hahn, C.; Jaramillo, T. F.; Bell, A. T. Electrochemical CO_2 reduction over compressively strained CuAg surface alloys with enhanced multi-carbon oxygenate selectivity. *J. Am. Chem. Soc.* **2017**, *139*, 15848−15857.

(11) He, J.; Johnson, N. J. J.; Huang, A.; Berlinguette, C. P. Electrocatalytic alloys for CO_2 reduction. *ChemSusChem* **2018**, *11*, 48−57.

(12) Hori, Y.; Konishi, H.; Futamura, T.; Murata, A.; Koga, O.; Sakurai, H.; Oguma, K. Deactivation of copper electrode" in electrochemical reduction of CO_2. *Electrochim. Acta* **2005**, *50*, 5354−5369.

(13) Xie, J.-F.; Huang, Y.-X.; Li, W.-W.; Song, X.-N.; Xiong, L.; Yu, H.-Q. Efficient electrochemical CO_2 reduction on a unique chrysanthemum-like Cu nanoflower electrode and direct observation of carbon deposite. *Electrochim. Acta* **2014**, *139*, 137−144.

(14) Jermann, B.; Augustynski, J. Long-term activation of the copper cathode in the course of CO_2 reduction. *Electrochim. Acta* **1994**, *39*, 1891−1896.

(15) Najafpour, M. M.; Fekete, M.; Sedigh, D. J.; Aro, E.-M.; Carpentier, R.; Eaton-Rye, J. J.; Nishihara, H.; Shen, J.-R.; Allakhverdiev, S. I.; Spiccia, L. Damage management in water-oxidizing catalysts: from photosystem II to nanosized metal oxides. *ACS Catal.* **2015**, *5*, 1499−1512.

(16) Kanan, M. W.; Nocera, D. G. In situ formation of an oxygen-evolving catalyst in neutral water containing phosphate and Co2+. *Science* **2008**, *321*, 1072−1075.

(17) Huynh, M.; Bediako, D. K.; Nocera, D. G. A functionally stable manganese oxide oxygen evolution catalyst in acid. *J. Am. Chem. Soc.* **2014**, *136*, 6002−6010.

(18) Gong, H.; Cao, X.; Li, F.; Gong, Y.; Gu, L.; Mendes, R. G.; Rummeli, M. H.; Strasser, P.; Yang, R. PdAuCu nanobranch as self-repairing electrocatalyst for oxygen reduction reaction. *ChemSusChem* **2017**, *10*, 1469−1474.

(19) Liu, J.; Zhang, Y.; Lu, L.; Wu, G.; Chen, W. Self-regenerated solar-driven photocatalytic water-splitting by urea derived graphitic carbon nitride with platinum nanoparticles. *Chem. Commun.* **2012**, *48*, 8826−8828.

DOI: 10.1021/acs.inorgchem.8b02311
Inorg. Chem. XXXX, XXX, XXX−XXX

(20) Dincă, M.; Surendranath, Y.; Nocera, D. G. Nickel-borate oxygen-evolving catalyst that functions under benign conditions. *Proc. Natl. Acad. Sci. U. S. A.* **2010**, *107*, 10337−10341.
(21) Lutterman, D. A.; Surendranath, Y.; Nocera, D. G. A self-healing oxygen-evolving catalyst. *J. Am. Chem. Soc.* **2009**, *131*, 3838−3839.
(22) Cobo, S.; Heidkamp, J.; Jacques, P.-A.; Fize, J.; Fourmond, V.; Guetaz, L.; Jousselme, B.; Ivanova, V.; Dau, H.; Palacin, S.; et al. A janus cobalt-based catalytic material for electro-splitting of water. *Nat. Mater.* **2012**, *11*, 802−807.
(23) Barroso, M.; Pendlebury, S. R.; Cowan, A. J.; Durrant, J. R. Charge carrier trapping, recombination and transfer in hematite (α-Fe_2O_3) water splitting photoanodes. *Chem. Sci.* **2013**, *4*, 2724−2734.
(24) Klahr, B.; Gimenez, S.; Fabregat-Santiago, F.; Bisquert, J.; Hamann, T. W. Photoelectrochemical and impedance spectroscopic investigation of water oxidation with "Co–Pi"-coated hematite electrodes. *J. Am. Chem. Soc.* **2012**, *134*, 16693−16700.
(25) Kwon, G.; Kokhan, O.; Han, A.; Chapman, K. W.; Chupas, P. J.; Du, P.; Tiede, D. M. Oxyanion induced variations in domain structure for amorphous cobalt oxide oxygen evolving catalysts, resolved by X-ray pair distribution function analysis. *Acta Crystallogr., Sect. B: Struct. Sci., Cryst. Eng. Mater.* **2015**, *71*, 713−721.
(26) Nocera, D. G. Chemistry of Personalized Solar Energy. *Inorg. Chem.* **2009**, *48*, 10001−10017.
(27) Wuttig, A.; Surendranath, Y. Impurity ion complexation enhances carbon dioxide reduction catalysis. *ACS Catal.* **2015**, *5*, 4479−4484.
(28) Jeon, H.; Kunze, S.; Scholten, F.; Cuenya, B. Prism-Shaped Cu Nanocatalysts for Electrochemical CO_2 Reduction to Ethylene. *ACS Catal.* **2018**, *8*, 531−535.
(29) Schreier, M.; Héroguel, F.; Steier, L.; Ahmad, S.; Luterbacher, J.; Mayer, M.; Luo, J.; Gratzel, M. Solar conversion of CO_2 to CO using Earth-abundant electrocatalysts prepared by atomic layer modification of CuO. *Nat. Energy* **2017**, *2*, 17087.
(30) Li, C. W.; Kanan, M. W. CO_2 reduction at low overpotential on Cu electrodes resulting from the reduction of thick Cu_2O films. *J. Am. Chem. Soc.* **2012**, *134*, 7231−7234.
(31) Tarasov, K. A.; O'Hare, D.; Isupov, V. P. Solid-State Chelation of Metal Ions by Ethylenediaminetetraacetate Intercalated in a Layered Double Hydroxide. *Inorg. Chem.* **2003**, *42*, 1919−1927.
(32) Kuhl, K. P.; Cave, E. R.; Abram, D. N.; Jaramillo, T. F. New insights into the electrochemical reduction of carbon dioxide on metallic copper surfaces. *Energy Environ. Sci.* **2012**, *5*, 7050−7059.
(33) Kuhl, K. P.; Hatsukade, T.; Cave, E. R.; Abram, D. N.; Kibsgaard, J.; Jaramillo, T. F. Electrocatalytic conversion of carbon dioxide to methane and methanol on transition metal surfaces. *J. Am. Chem. Soc.* **2014**, *136*, 14107−14113.
(34) Reller, C.; Krause, R.; Volkova, E.; Schmid, B.; Neubauer, S.; Rucki, A.; Schuster, M.; Schmid, G. Selective electroreduction of CO_2 toward ethylene on nano dendritic copper catalysts at high current density. *Adv. Energy Mater.* **2017**, *7*, 1602114.
(35) Dutta, A.; Rahaman, M.; Mohos, M.; Zanetti, A.; Broekmann, P. Electrochemical CO_2 conversion using skeleton (Sponge) type of Cu catalysts. *ACS Catal.* **2017**, *7*, 5431−5437.
(36) Sen, S.; Liu, D.; Palmore, G. T. R. Electrochemical reduction of CO_2 at copper nanofoams. *ACS Catal.* **2014**, *4*, 3091−3095.
(37) Zhu, S.; Jiang, B.; Cai, W.-B.; Shao, M. Direct observation on reaction intermediates and the role of bicarbonate anions in CO_2 electrochemical reduction reaction on Cu surfaces. *J. Am. Chem. Soc.* **2017**, *139*, 15664−15667.
(38) Dettelbach, K. E.; Kolbeck, M.; Huang, A.; He, J.; Berlinguette, C. P. Rapid quantification of film thickness and metal loading for electrocatalytic metal oxide films. *Chem. Mater.* **2017**, *29*, 7272−7277.
(39) Speck, F. D.; Dettelbach, K. E.; Sherbo, R. S.; Salvatore, D. A.; Huang, A.; Berlinguette, C. P. On the electrolytic stability of iron-nickel oxides. *Chem.* **2017**, *2*, 590−597.
(40) Peterson, A. A.; Abild-Pedersen, F.; Studt, F.; Rossmeisl, J.; Nørskov, J. K. How copper catalyzes the electroreduction of carbon dioxide into hydrocarbon fuels. *Energy Environ. Sci.* **2010**, *3*, 1311−1315.

DOI: 10.1021/acs.inorgchem.8b02311
Inorg. Chem. XXXX, XXX, XXX−XXX